# On the joint exploitation of long-term DInSAR time series and geological information for the investigation of ground settlements in the town of Roma (Italy)

Remote Sensing of Environment

# On the joint exploitation of long-term DInSAR time series and geological information for the investigation of ground settlements in the town of Roma (Italy)

S. Scifoni [a,*], M. Bonano [b], M. Marsella [a], A. Sonnessa [a], V. Tagliafierro [a], M. Manunta [b], R. Lanari [b], C. Ojha [b], M. Sciotti [a]

[a] *Università di Roma "Sapienza", Dipartimento di Ingegneria, Civile, Edile e Ambientale (DICEA), Via Eudossiana 18, 00184 Roma, Italy*
[b] *Istituto per il Rilevamento Elettromagnetico dell'Ambiente - Consiglio Nazionale delle Ricerche (IREA-CNR), Via Diocleziano 328, 80124 Napoli, Italy*

a r t i c l e i n f o

*Article history:*

*Keywords:*
SBAS-DInSAR
Deformation time series
Ground settlements
Geological setting

a b s t r a c t

In this work the long-term deformation time series have been jointly exploited with the geological information and the structural characteristics of the buildings, in order to study the interactions between the soils and the man-made structures and to investigate the response of different buildings to the settlements.
The presented analysis has been carried out by applying the advanced multi-temporal DInSAR technique referred to as (SBAS approach to a SAR dataset, collected over the town of Roma(Italy) il.
The obtained SBAS-DInSAR measurements, analysized in light of the geological setting and the spatial distribution of the settlements, indicate that the observed displacements are mainly linked to a residual consolidation process, correlated with the urbanization and hydrometric level of the Tevere River. The local variation in the deformation rates can be related to the intrinsic variability of the soils filling the alluvial valley and to time since loading application.



## 1. Introduction

The quantitative evaluation of the effects of soil settlements on buildings is traditionally based on in-situ surveying techniques able to measure sub-centimetre displacements of benchmarks installed on the selected structures. In the last decades, the extensive use of satellite remote sensing data, such as Synthetic Aperture Radar (SAR) images, has represented an important breakthrough in the context of non-invasive ground deformation analyses over large areas, thanks to their large spatial coverage capability and relatively short revisit times, as well as to their medium/high spatial resolution. In this context, the Differential SAR Interferometry (DInSAR) technology (Gabriel, Goldstein, & Zebker, 1989; Massonnet & Feigl, 1998; Burgmann et al., 2000) allows us to map and measure deformation phe-nomena due to both natural and man-made causes (Massonnet et al., 1993; Massonnet, Briole, & Arnaud, 1995; Peltzer and Rosen, 1995; Tesauro et al., 2000), with limited monitoring costs compared to the traditional in situ surveys. DInSAR is based on the exploitation of the phase difference (interferogram) between two temporally separated SAR images, thus retrieving information on the sensor Line of Sight (LOS) projection of the detected displacements occurred between the two acquisition times. Furthermore, the use of advanced DInSAR approaches (Ferretti, Prati, & Rocca, 2000; Berardino, Fornaro, Lanari, & Sansosti, 2002; Mora et al., 2003; Werner, Wegmüller, Strozzi, & Wiesmann, 2003; Lanari et al., 2004; Ferretti et al., 2011), based on the exploitation of SAR acquisition sequences collected over large time spans, allows providing useful information on both the spatial and the temporal patterns of the detected displacements through the generation of time series, with centimetre to millimetre accuracy (Casu, Manzo, & Lanari, 2006; Lanari, Casu, Manzo, & Lundgren, 2007; Bonano, Manunta, Pepe, Paglia, & Lanari, 2013).

DInSARremote sens- ing techniques have also demonstrated the capability to provide valu- able information on the displacements affecting single buildings (Lanari et al., 2004; Bonano, Manunta, Marsella, & Lanari, 2012, Bru et al., 2013). In such a context, advanced DInSAR techniques can be cru- cial for the analysis of the static behaviour of civil structures during ex- cavation or consolidation works (Dixon et al., 2006; Sansosti et al., 2014; Tomás et al., 2012) in comparison with not-perturbed conditions. Inparticular, thanks to the capability to extend backwards the DInSAR in- vestigations by exploiting the SAR data archives available since the early ERS-1 ESA mission in 1992, it is possible to perform long-term deforma- tion analyses (Bonano et al., 2012) and compare pre- with post-eventconditions (Tomás et al., 2010; Sanabria et al., 2014). This information may significantly contribute to the implementation of damage assess- ment analyses and to the evaluation of risk scenarios (Burland & Wroth, 1974;

* Corresponding author at: D.I.C.E.A. - Università di Roma "Sapienza", Via Eudossiana,18, 00184 Roma, Italy.

Mroueh & Shahrour, 2003; Ardizzone et al., 2012; Arangio et al., 2013; Sanabria et al., 2014). In addition, by providing a dense spatial data sampling on the ground, compared to that achievable by standard in situ monitoring approaches, and a quite regular temporal sampling (from monthly, ERS/ENVISAT missions, to a few days revisit time, TerraSAR-X, COSMO-SkyMed and Sentinel-1 constellations), DInSAR measurements can also represent a valuable resource to cali- brate and validate models for structure damage assessment (Arangioet al., 2013), as well as to understand the evolution of soil consolidation processes (Cascini, Ferlisi, Fornaro, Peduto, & Manunta, 2007; Manunta et al., 2008; Stramondo et al., 2008; Tomás et al., 2010).

Nevertheless, in urban contexts the scientific community has been more devoted to the exploitation of DInSAR technology to detect, map and follow the temporal behaviour of ground deformations and to investigate their effects on buildings and structures, rather than to study and understand the possible causes of the observed displacements and the related soil-structure interactions.

This work investigates how long-term satellite DInSAR deformation time series relevant to urban areas can be jointly exploited with the geological information and the structural characteristics of the investigated buildings, in order to study the interactions between the soils and the man-made structures and to examine the response of different buildings to the settlements. In particular, the presented analysis has been carried out by applying the advanced DInSAR technique referred to as Small BAseline Subset (SBAS) approach to an ERS/ENVISAT satellite SAR dataset, collected during the 1992-2010 time interval over the town of Roma (Italy). The retrieved SBAS-DInSAR measurements have been combined with the geological setting and the structural characteristics of the buildings, aimed at investigating the deformation causes and evaluating the variation in magnitude of the settlements at the scale of single building. The analysis has been performed first at a large spatial scale relevant to the Tevere valley; subsequently, a local scale study has been performed in the central area of Roma focusing on two zones located at the West and East sides of the Tevere River, aimed at investigating the correlation between possible triggering factors and the measured subsidence rates.

## 2. Rationale of the SBAS-DInSAR technique

As previously stated, DInSAR is based on the exploitation of the phase difference (interferogram) between two temporally separated SAR images, which allows us to retrieve information on the sensor Line-Of-Sight (LOS) projection of the detected displacements occurred between the two acquisition times. Furthermore, the use of advanced DInSAR approaches (Ferretti et al., 2000; Berardino et al., 2002; Werner et al.,

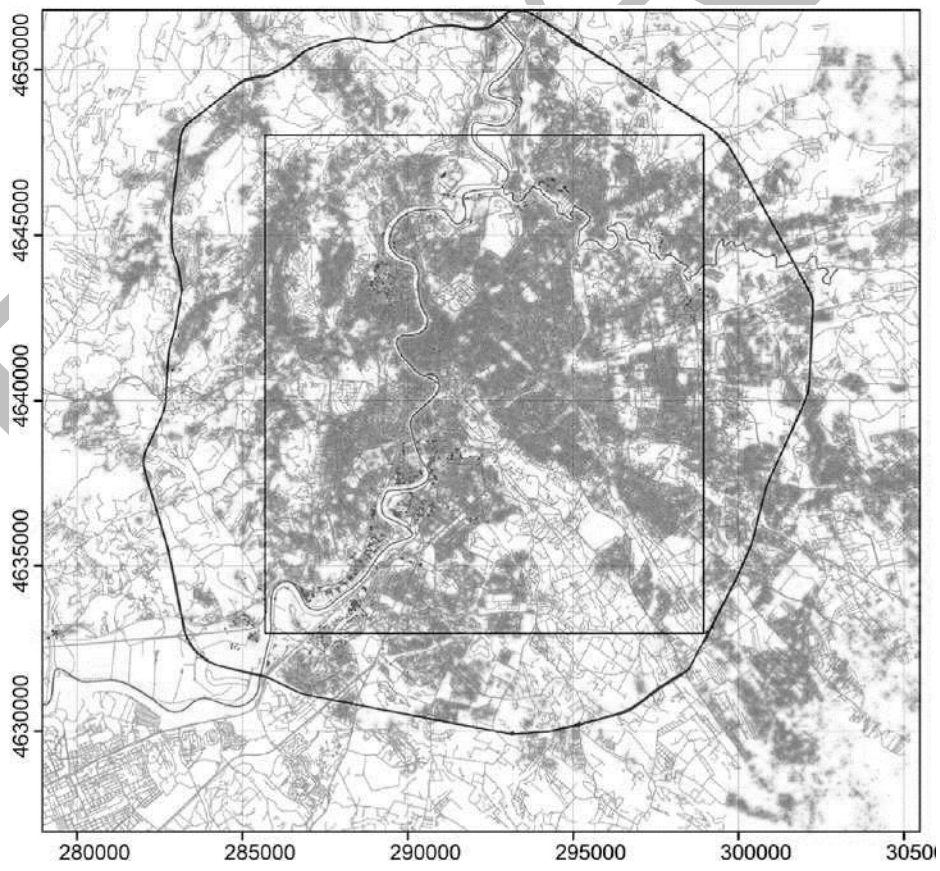


Fig. 1. Thematic layers obtained as output products from the implemented data analysis procedure: cumulative displacement map, relevant to the ERS-ENVISAT SBAS-DInSAR analysis between 1992 and 2010, superimposed on a map of the urban area of Roma (Italy). The black rectangle highlights the area mainly interested by deformation phenomena.

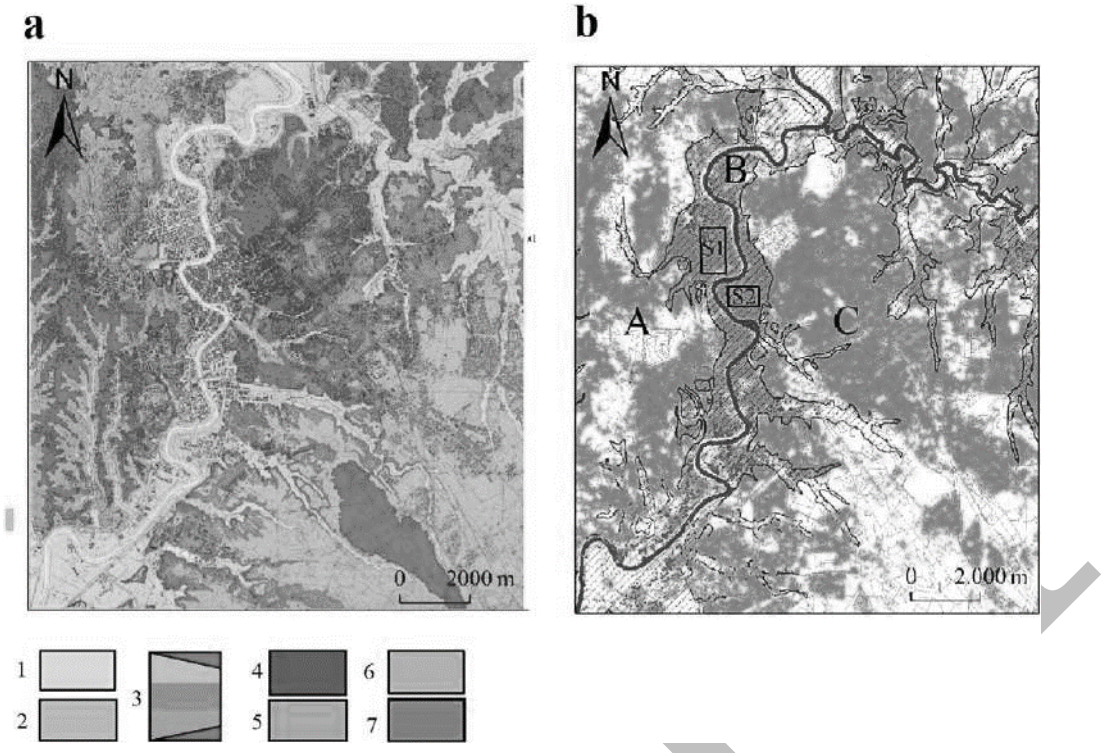


Fig. 2. a) Geological map (Ventriglia & Sciotti, 1970a), relevant to the black rectangle in Fig. 1, evidencing the actual path of the Tevere River bordered by alluvial Holocenic deposits. 1) Alluvial deposits (Holocene)–2) terraced fluvial deposits (Middle Pleistocene)–3) pyroclastic flows and lava flows of Colli Albani Volcano–4) fallout thepra of Monti Sabatini volcano–5) fluvio-lacustrine sediments (Middle Pleistocene- Lower Pleistocene)–6) infralittoral and fluvial–deltaic sediments (Middle Pleistocene-Lower Pleistocene)–7) marine grey clays alternated with fine sands (Upper Pliocene); 2b) zoom of the cumulative displacement map detected through the SBAS-DInSAR analysis. The evidenced area identifying the alluvial deposits, the city map of Roma, the Tevere and the Aniene River paths are indicated. The two insets referred to as S1 and S2, corresponding to the areas investigated in detail in this work, are highlighted. "A" corresponds to the Monte Mario and Gianicolo Hills, whereas "B" indicates the Tevere alluvial plain crossing the town along the NS direction; the area "C" to the eastern side, corresponding to the wide volcanic Plateau of the Colli Albani.

2003; Lanari et al., 2004; Ferretti et al., 2011), based on the exploitation of large multi-temporal SAR datasets, allows providing useful information on both the spatial and temporal patterns of the detected displacements through the generation of time series, with centimetre to millimetre accuracy (Casu et al., 2006; Lanari et al., 2007; Bonano et al., 2013).

The multi-temporal SBAS-DInSAR technique (Berardino et al., 2002; Lanari et al., 2004) permits to investigate and map ground movements through the generation of mean deformation velocity maps and corresponding displacement time series. It relies on a proper selection of a large number of SAR image pairs characterized by short spatial and temporal separations (baseline) between the acquisition orbits, in order to mitigate decorrelation phenomena (Zebker & Villasenor, 1992), and to maximise the number of reliable SAR measure points. Differently from other advanced multi-temporal DInSAR techniques, the SBAS approach does not need any a-priori information on the investigated ground deformation phenomena, thus representing a valuable method to detect and measure non-linear LOS displacements over time. Furthermore, the SBAS-DInSAR technique is capable to deal with multi-sensor SAR data, acquired by different radar systems but geometrically compatible (i.e. with same characteristics of the illumination geometry) as for the case of ERS-1/2 and ENVISAT sensors (Bonano et al., 2012). Such a multi-sensor approach allows guaranteeing the continuity in the monitoring of the Earth's surface deformation phenomena by generating LOS displacement maps and associated time series spanning very long periods (decades), providing unprecedented information for studying long-term ground movements. It is worth noting that the multi-temporal SBAS technique has been deeply assessed in several deformation contexts, retrieving an accuracy of about 5 mm for the single deformation measurements and 1 mm/year for what concerns the mean deformation velocity information (Bonano et al., 2012; Bonano et al., 2013; Zeni et al., 2011).

As a result, the multi-sensor SBAS technique is an effective tool able to fully exploit the existing archives of the European Space Agency (ESA), with a rather limited loss of coherent points with respect to the single sensor case (Bonano et al., 2012).

## 3. Wide area SBAS-DInSAR analysis applied to the town of Roma

The DInSAR dataset consists of 91 ERS-1/2 and 40 ENVISAT data, acquired over descending orbits from June 1992 to July 2007, and from November 2002 to January 2010, respectively. These SAR images were combined to generate 352 differential interferograms with spatial and temporal baseline values less than 400 m and 1550 days, respectively, to be processed through the SBAS approach. The deformation phenomena within the urban area of Roma have already been investigated (Manunta et al., 2008; Stramondo et al., 2008; Zeni et al., 2011; Tapete, Fanti, Cecchi, Petrangeli, & Casagli, 2012) through the analysis of large stacks of SAR images. In this work, we show the results obtained through the SBAS-DInSAR analysis performed on the complete ERS/–ENVISAT descending orbit archive (1992-2010) focusing on the central area of the city.

The SBAS-DInSAR measurements were analysed in a 3D GIS environment, suitable to localize, visualize and spatially correlate the observed displacements with the geological setting and compared with the cumulated iso-displacement maps and profiles (LOS component) interpolated by applying a Universal Kriging approach (Matheron, 1963).

The used Kriging interpolation was assessed by calculating, for each single coherent pixel, the error between the original SBAS measurement, cumulated during the analysed time interval, and the spatially-

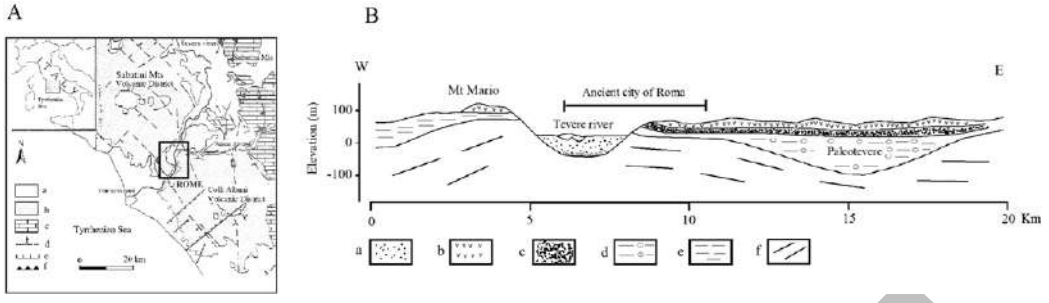


Fig. 3. A) Geological scheme of the area surrounding Roma. a) Messinian to Holocene sediments; b) Pleistocene lavas and volcaniclastics; c) Mesozoic to Cenozoic sediments; d) main buried faults; e) normal faults; f) thrust faults (modified from Sagnotti et al., 1994). B) Schematic geological profile of the ancient town of Roma. a) silts, sands and clays of the current Tevere River valley (Holocene); b) pyroclastic deposits of the Colli Albani and Sabatini Mountains volcanic districts (Middle Pleistocene); c) fluvial-lacustrine deposits (Middle Pleistocene); d) fluvial and lacustrine sediments of the Paleotevere (Middle Pleistocene); e) infralittoral and fluvial-deltaic sediments (Middle Pleistocene–Lower Pleistocene); f) Marine grey clays, alternated with fine sands (Upper Pliocene).

interpolated value. The retrieved statistics show the mean and the standard deviation values, which correspond to 0.02 cm and 1.15 cm, respectively. Since our long-term SBAS measurements are relevant to a period of 18 years, we can reasonably assume that the error between the original and the interpolated SBAS measurements is around 0.5 mm/year. Since the SBAS accuracy is 1 mm/year for what concerns the mean deformation velocity information, the error introduced by the interpolation operation can be considered negligible.

We remark that the considered SBAS-DInSAR measurements are LOS-projected and do not allow us to retrieve information on the vertical and the East-West displacement components. However, since there are no major evidences of horizontal displacement components, we can reasonably assume that the investigated displacements are mainly vertical, thus neglecting significant East-West components. Therefore, we can use LOS measurements to investigate the detected ground settlements.

Fig. 1 shows an overview of the cumulative LOS displacement map for the whole metropolitan city of Roma that is characterized by a predominance of stable areas having not significant rates (points coloured in green correspond to rates ranging ±2 mm/year). On the contrary, long-term ground settlement processes are quite marked in the areas in proximity of the path of the Tevere River and depicted by points coloured in yellow to dark red (from 2 to about 10 mm/year).

Focusing on the central areas, the comparison with the geological map (Fig. 2a) and the DInSAR cumulated LOS displacement velocity (Fig. 2b) shows a clear correlation between the distribution of alluvial deposits (along the main and the subsidiary flooding plains) and the observed deformation pattern.

The buildings located along the alluvial plain appear affected by settlement processes, which are more conspicuous with respect to other areas but still varying spatially in their intensity.

Therefore, the results of the SBAS-DInSAR analysis are compared to the conditioning factors for ground settlements in each investigated area, which are linked to the characteristics and geologic age of the underground terrains, as well as to geotechnical and hydrological aspects. A detailed analysis is carried out in the two areas S1 and S2, situated on the western and eastern side of the Tevere River, respectively, and delimited by the rectangular insets in Fig. 2b.

## 4. Geological setting of the urban area of Roma

The overall geological setting of the area of Roma is well-known and widely described in the literature (Ventriglia & Sciotti, 1970a; Marra & Rosa, 1995; Ventriglia, 2002; Funiciello & Giordano, 2008). A large number of soil investigations and geologic logs collected since 1960 are available to analyse the underground setting of the whole area and to reconstruct the stratigraphic succession of the alluvial deposits, as presented in the following. The 1:20,000 scale geological map, compiled by Ventriglia and Sciotti (1970a), provides a general view of the area

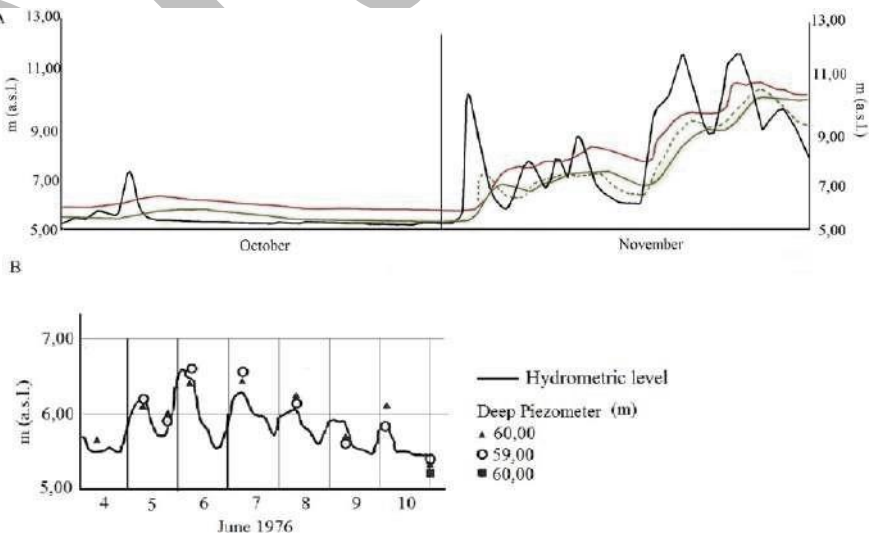


Fig. 4. Comparison between the variations of the hydrometric and piezometric levels relevant to the alluvial sediments; (A) hydrometric and piezometric levels in correspondence to shallower sandy layers in ordinary regime (October) and ordinary overflow conditions (November) (as modified by Ministero dei Lavori Pubblici, 1901). Black line indicates the hydrometric level, whereas the continuous, dashed green and red lines represent the piezometric levels; (B) hydrometric and piezometric levels in correspondence to gravel layers in ordinary regime (June) (modified by Calabresi, Cassinis, & Nisio, 1980).

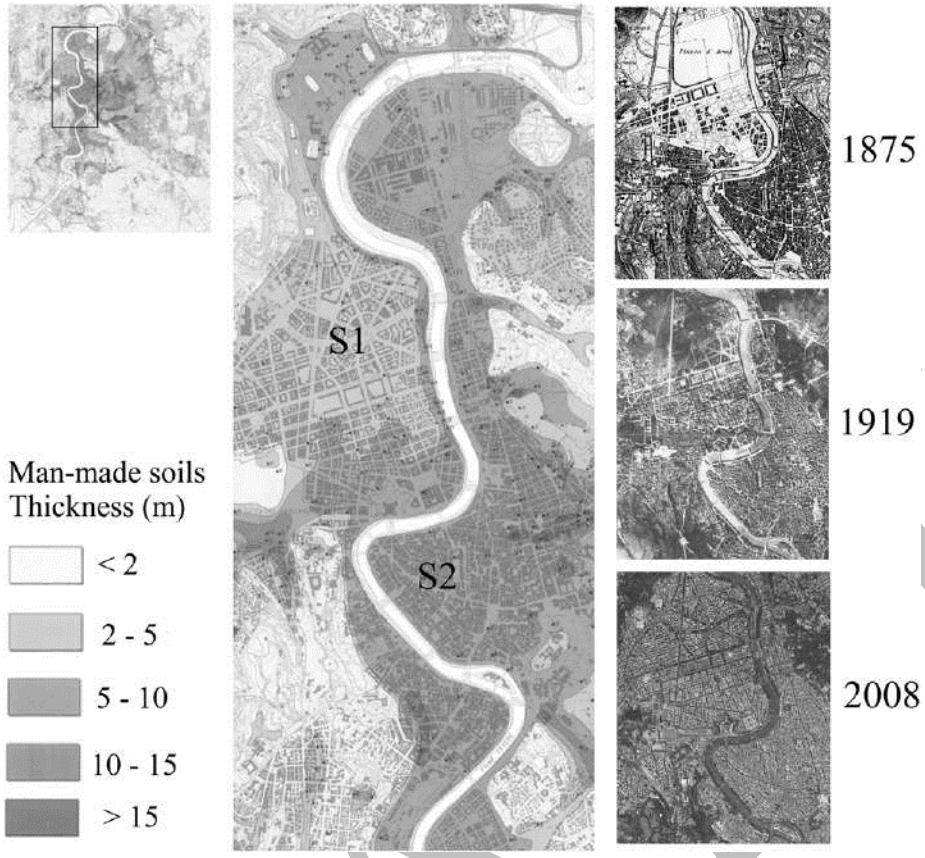


Fig. 5. Man-made soils thickness map (Ventriglia & Sciotti, 1970b) on the left. On the right, the urbanization process of the two studied areas. 1875 IGM map at 1:25,000 scale, 1919 aerial photo (Frutaz A.P., 1972), 2008 orthophoto (from Ministero dell'Ambiente e della tutela del territorio e del mare).

under investigation including all the information relevant to the discussion of the results.

The town of Roma is located within the area of the lower Tevere River valley between the Colli Albani Volcanic district to the southeast and the Sabatini Mountains Volcanic District to the northwest (Fig. 3).

The morphology and the stratigraphy of the area where most of the town was built up are the consequence of a combination of tectonic, volcanic, fluvial and lacustrine sedimentation, as well as of the erosion processes that alternated from the upper Pliocene to the Holocene. In the geological map of Fig. 2a (Ventriglia & Sciotti, 1970a) three sectors characterized by different stratigraphic successions are evidenced: the area "A", located at the West side of the Tevere River, corresponding to the Monte Mario and Gianicolo Hills (110 m a.s.l.); the area "B", elongated toward the NS direction, which is representative for the Tevere alluvial plain; the area "C" to the eastern side that covers the wide volcanic Plateau of the Albani Hills engraved by the tributaries of the Tevere River. Along the slopes of the hills at the western side of the Tevere valley the Pliocenic marine clays outcrop: they represent the substratum of

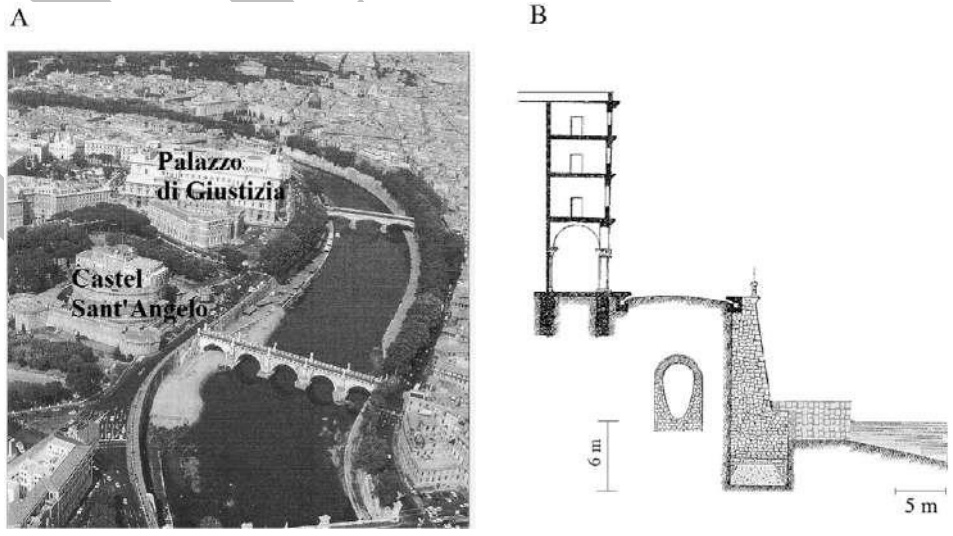


Fig. 6. A) Aerial photo of the Tevere River across the two studied areas (photo by Studio Arletti 1997); B) schematic view of the embankment walls built up between 1878 and 1900 (modified by Ministero dei Lavori Pubblici, 1901).

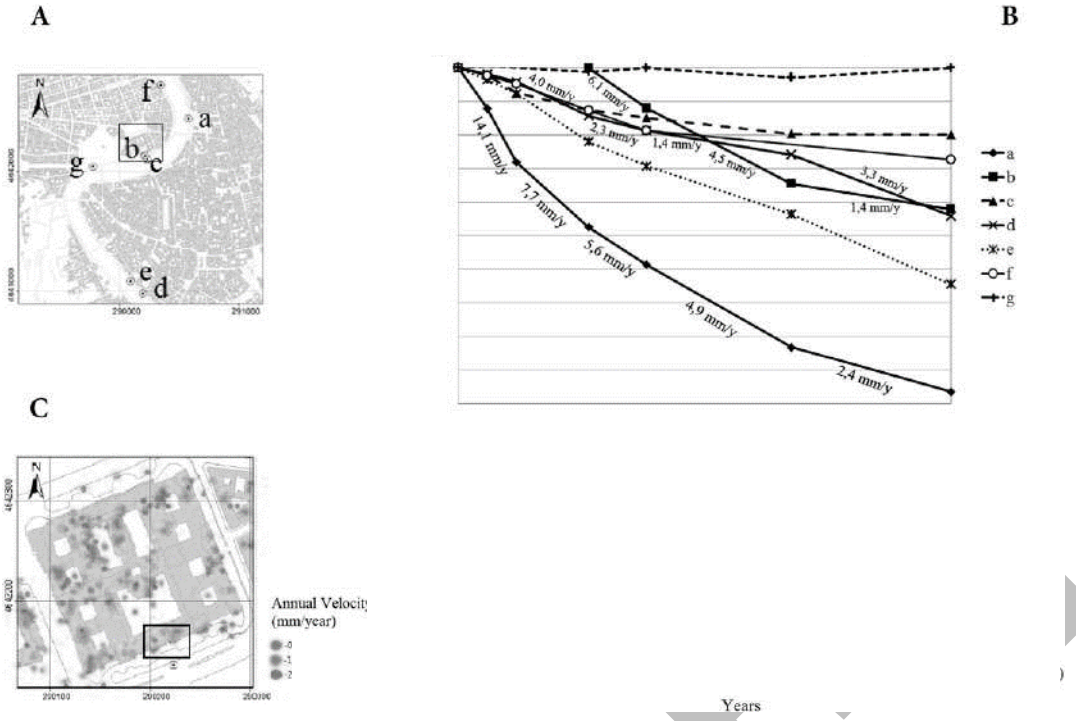


Fig. 7. A) Benchmark position, black box indicates Palazza di Giustizia; B) cumulative displacements obtained from levelling survey between 1902 and 1936 near the embankment walls and some buildings: a) Lungotevere di Ripetta; b) Palazzo di giustizia; c) Ponte Umberto (right side); d) Ponte Sisto; e) Lungotevere Tibaldi; f) Lungotevere dei Mellini; g) Castel Sant'Angelo; C) detailed view of cumulative displacement measurements of Palazzo di Giustizia from 1992 to 2010;

the whole urban area and have a thickness of some hundreds of metres. On the top of the hill, marine sediments are covered by littoral and fluvial deposits of the lower and middle Pleistocene and, finally, by pyroclastic terrain of the Monte Sabatini volcano.

At the East side of the Tevere Valley, the Pliocenic terrains can be found at a very large depth from the surface, since they were deeply eroded (down to about 100 m below the present sea level) by an important precursor of the current river, the "Paleotevere" (Fig. 3). In the middle Pleistocene, the Paleotevere valley has been gradually filled at first by a very thick layer of fluvial and lacustrine sediments (from gravels to clays) and, subsequently, by the pyroclastic deposits of the Colli Albani volcano. The volcanic deposits produced the obstruction of the Paleotevere valley and, during the last period of the lowering of the sea level (Wurmian glaciation occurred about 18,000 years ago), the river has turned its track toward West, deeply eroding the volcanic and sedimentary layers along the present-day valley (up to 40 m below the current sea level).

The raise of the sea level up to the current one has produced the gradual filling of the new valley and the consequent formation of the present-day Tevere alluvial plain (corresponding to the area "B" in Fig. 2b). The sediments filling the most recent Tevere valley have now reached an overall thickness of about 50 m and are mainly formed by silty clays and organic clays, with scattered levels of sandy-silts and sands. At the base of the medium-fine grain size sediments, an extended layer of sands and gravels having a thickness between 4 and 10 m, crosses the whole valley.

From a hydrogeological point of view, in the eastern part (C) of the study area, the main aquifer rests within the Pleistocenic sediments and in the upper volcanites of the Albani Hills flowing in the direction of the Tevere, while in the western part (A) it rests within the Pleistocenic sediments and flowing toward South. In the recent alluvial deposits (B), the aquifer is compounded by a shallower unconfined unit of fine grain size sediments, which is characterized by a low permeability coefficient and a water table level at a few metres of depth, and a confined aquifer formed by gravels having a permeability ranging from $10^{-4}$ to $10^{-5}$ m/s.

## 5. Settlement in the alluvial plain

Long-term ground settlements affect the buildings located along the alluvial plain of the Tevere River, where the conditioning factor is the presence of compressible soils below the water table level. The triggering factors can be both the variation of the piezometric levels, due to natural or anthropic causes, and the application of external loads due to the town expansion (construction of buildings and accumulation of man-made fills to level the ground surface). The two factors can either act independently or jointly, in space and time, also in relation to the distribution and thickness of the alluvial deposits.


Fig. 8. Palazzo di Giustizia. Comparison between displacements and hydrometric level in ordinary regime between 1971 and 1972.
Modified by Calabresi et al. (1980)

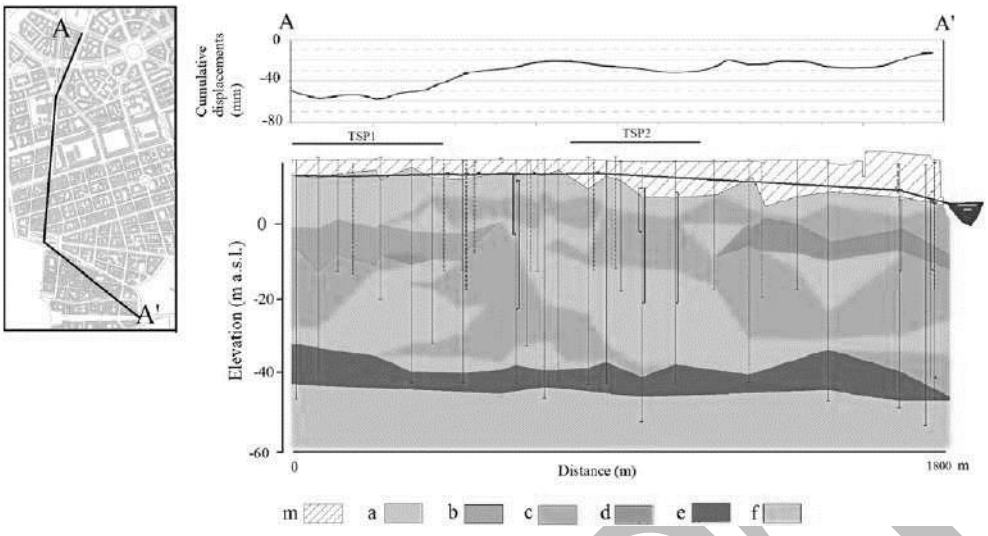


Fig. 9. Geological profile along S1 and section of the cumulative displacements observed with DInSAR. m) Man-made soil; a) silty clay; b) organic silty clay, with thin layers of peat; c) sandy silt with thin layers of clay; d) medium to fine sand and sandy silts; e) sandy gravel; f) marine grey clays alternated with fine sands (Upper Pliocene). The horizontal dark blue line indicates the piezometric level; the vertical blue line shows the borehole location. To highlight the stratigraphic succession the vertical axis scale is 10 times higher than the horizontal one.

### *5.1. The aquifer regime*

On the overall the hydrogeological pattern does not present significant variations among different areas of the alluvial plain. The groundwater regime is strongly correlated to the cyclic seasonal fluctuations of the river: piezometers located in shallower sandy layers evidence that the piezometric levels tend to follow, with some deviation, the hydrometric levels (Fig. 4A), whereas those located within the gravels respond almost instantaneously to the river level variations (Fig. 4B).

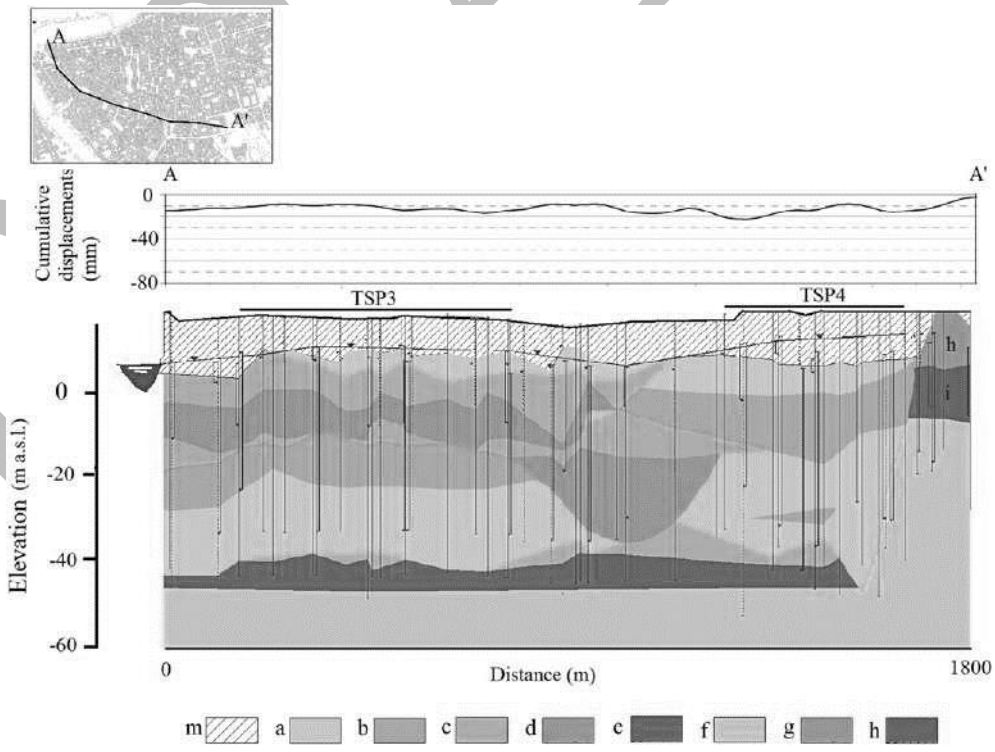


Fig. 10. Geological profile along S2 area and section of cumulative displacements observed with DInSAR. m) Man-made soil; a) silty clay; b) organic silty clay, with thin layers of peat; c) sandy silts with thin layers of clay; d) medium to fine sand and sandy silt; e) sandy gravel; f) marine grey clays alternated with fine sands (Upper Pliocene); g) sand and silty sand (Middle Pleistocene); h) sandy gravel (Middle Pleistocene). The horizontal dark blue line indicates the piezometric level; the vertical blue line shows the borehole location. To highlight the stratigraphic succession the vertical axis scale is 10 times higher than the horizontal one.

The river level measured at the hydrometer located in the central area of the town oscillates between 5.5 and 7 m in ordinary regime, reaching 10-13 m in ordinary overflow conditions and exceeding 16 m in extraordinary flooding periods. During the November 1893 flooding event, the hydrometric level reached 12 m a.s.l., whereas the piezometric level increased about 4-5 m in three boreholes located at about 100 m from the river (Fig. 4A) (Ministero dei lLavori Pubblici, 1901). Similarly, during the 2010 flooding event characterized by a hydrometric level of 10.5 m, new instruments installed in proximity of the already existing ones showed that the variation of the piezometric level is more significant within the coarse grained soils (uplift of 2-3 m) than in the finer soils (few decimetres). Regarding the variation of the hydrometric level, it is worth noting that the annual values in the period 1945-1960 have been fluctuating between 6 and 7 m a.s.l. (on average 6.4 m a.s.l.). Since 1970 a lowering trend has been recorded, reaching 5.60 m a.s.l. in the period 1993–2008, as testified by the average annual value measured by the regional hydrography department (data from Ufficio Idrografico and Mareografico of Lazio Region).

Regarding the evolution of the piezometric level it is worth noting that in the town of Roma a fixed network of instruments to provide systematic measurements is not installed. For this reason, the information is only available on limited areas and for time spans preceding and contemporary to the SBAS-DInSAR measurements. On the overall, by comparing the older (beginning 1900) and the more recent (1963 to 2010) available measurements, the differences do not appear noticeable, remaining confined in the order of seasonal fluctuations, which is 1-2 m. Thus, the monitoring of piezometric levels does not allow distinguishing the superimposition of the two phenomena above described: the seasonal fluctuations and the slow lowering of the river level. Well documented cases demonstrate that they both affect the trend of the piezometric level and the variations of the hydraulic head (Calabresi et al., 1980), which lead to the deformation of the most compressible layers and, consequently, to the settlements of a large number of buildings of different type and size located along the Tevere River.

### 5.2. The urbanization process

The expansion of the urban area in Roma has occurred gradually over a long time span: in the same areas it started a few centuries BCE lasting up to the 17th century, whereas in other areas between the19th and the first half of the 20th centuries. In the investigated areas, most of the buildings have a masonry structure and shallow foundations at a depth of −m from the ground surface. Up to the 19th century the foundations were continuous (concrete strip footing, beams and slabs) and later became discontinuous, like the shaft and arch foundations. The building elevations increased gradually with the number of floors (of about 3 m): 3 floors in the 15–16th centuries, from 5 to 6 floors during the 19th century and up to 10 floors in the first half of the 20th century. Many buildings have one or two additional levels in the basement and some were elevated for 1 or 2 floors many years after their construction. Only a few buildings, raised in the second half of the 20th century after the demolition of the pre-existing structures, have foundations on concrete piles working by toe resistance on the gravel layer at the base of the finer and soft soils.

Finally, it is worth mentioning that, since the first centuries of its development, the urbanization of the more ancient parts of the town and, mostly, of the alluvial plain has been accompanied by the raise of the original ground level. This was obtained through the emplacement of a continuous layer of man-made soils required, either to fill the marshland, or to restrict the flooding areas. The thickness of the man-made soils is variable along the different areas, ranging up to 15 m. In most cases the filling has preceded or accompanied the numerous urbanization phases; therefore, it has been carried out in subsequent stages, sometimes significantly spaced in time (Fig. 5). The layer of man-made ground contains the remnants of the ancient city and along the century many building was funded on structures of the roman age.

### 5.3. Settlements versus stratigraphy and urbanization

The availability of deformation time series, relevant to levelling surveys conducted on some structures built up at the end of the 19th century, allowed us to analyse the evolution of the settlements up to the first decades of the 20th century. Particularly relevant in our analysis are the data collected along the large embankment walls (Fig. 6), built up between 1878 and 1900 to protect the urban area against the frequent floods of the Tevere River.

High precision levelling surveys were initially conducted every two years and, then, every 10 years later up to 1936 (Aquilina, 1937). The analysis of the deformation trends observed between 1902 and 1936 on some significant points (Fig. 7A and B) highlights that the lowering is quite steady over time with a gradual decrease (benchmark a), although, in some cases, following a long stable period, it may significantly accelerate (benchmark d). The benchmarks located at a few hundred metre distance along the walls (benchmarks a, f and c) show significant differences in the magnitude (from a few centimetres to two decimetres), linked to the different thickness of the underneath compressible soils.

The more stable points, as in the case of benchmark g located in correspondence to Castel S. Angelo (Fig. 6), correspond to very ancient structures that have just little displacements. The huge structure of Castel Sant' Angelo was built up during different stages between 393 and the second half of the 500, and founded over a more ancient structure, the Mausoleo of Adriano, built between 123 and 136. Particularly remarkable is the deformation trend observed in correspondence to

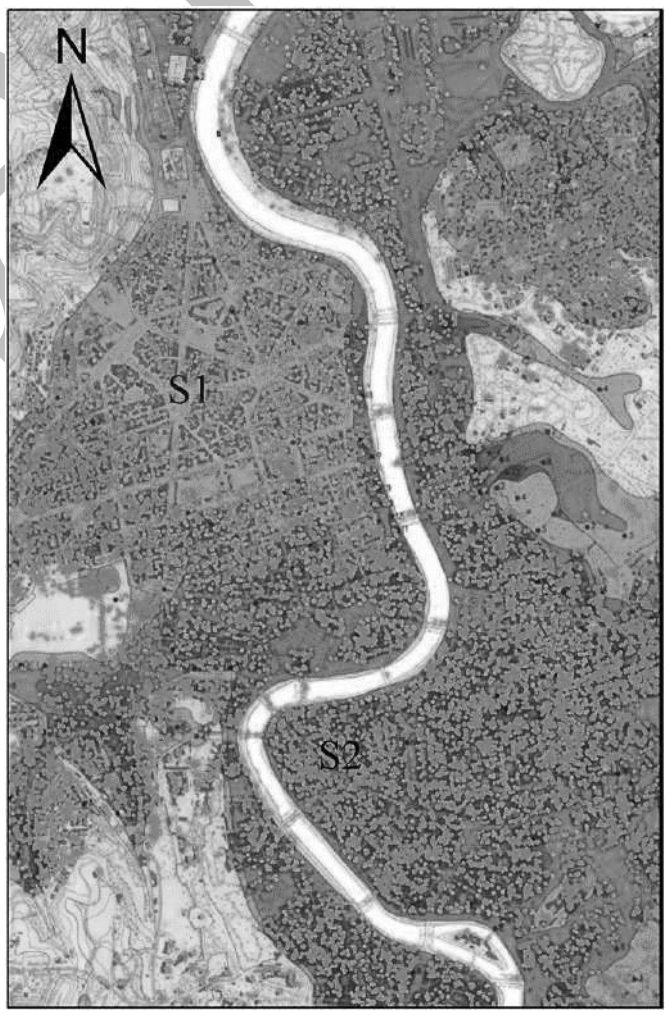


Fig. 11. Man-made soils thickness map with overlapped the cumulative displacements.

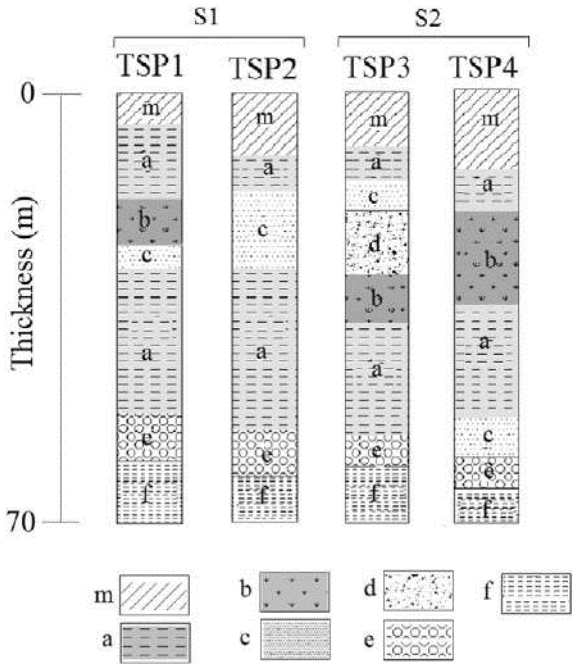


Fig. 12. Typical soil profiles. m) man-made soil; a) silty clay; b) organic silty clay with thin layer of peat; c) sandy silts with thin layers of clay; d) medium to fine sand and sandy silt; e) sandy gravel; f) marine grey clays alternated with fine sands (Upper Pliocene). Grey color highlights the more compressible layers. The cumulated settlements measured in S2 (ranging between about −20 and −30 mm) are significantly smaller than those of S1 (reaching about −70 to −80 mm).

benchmark b, located across from the huge Palazzo di Giustizia (Fig. 6). The building, built up between 1889 and 1899, has a rectangular plan of 170 × 154 m and rests on a wide foundation plateau of variable thickness (between 1.7 and 2.4 m), set at around 9 m a.s.l.

The measures relevant to benchmark b are available for a longer time period; in particular between 1925 and 1936, the settlements measured on the benchmark located in front of the building facing the riverbed, had an average velocity of 1.4 mm/year (Aquilina, 1937).

Between 1970 and 1972, the average settlement velocity of the whole structure, before the reinforcement of its foundations, was of about 2.8 mm/year, with larger displacement values in the frontal portion; Fig. 8 shows the comparison between the displacements and the hydrometric level in ordinary regime between 1971 and 1972. During the 1981-1983 time interval the average velocity value was 1.7 mm/year (Amanti, Gisotti, & Pecci, 1995).

Despite it is not possible to obtain a direct correlation between the SBAS-DInSAR time series and the levelling measurements, due to both the non-overlapping observation periods and their different accuracies, we performed a detailed analysis of the displacement time series related to the points located in the proximity of benchmark b (Fig. 7C). Fig. 7D pictures the plot relevant to the cumulative deformations estimated for the LOS component of DInSAR measurements, accounting for an average velocity of about 1 mm/year, which is in accordance with a decreasing phase of the settlement process.

In the following sections, in-depth reconstructions of the local stratigraphy of the alluvial plain in comparison with cumulative SBAS-DInSAR displacements along some sections, extrapolated in correspondence to single historical buildings, are extensively discussed. This analysis was possible thanks to the geological and hydrogeological investigations conducted between 1995 and 2008 for the project of a new metro line construction, which provided a large numbers of logs reaching a maximum depth of about 70 m b.s.l. By exploiting these data it was possible to extrapolate the detailed stratigraphic profiles in correspondence to two areas, namely S1 and S2 in Fig. 2 (Sciotti, 2010), which were compared to the corresponding cumulative settlement profiles (Figs. 9 and 10). For a better interpretation, the vertical axis is magnified 10 times with respect to the horizontal one.

The alluvial deposits overlying the deep gravel layers are rather variable in grading and include: (a) silty clay; (b) organic silty clay, with thin layers of peat; (c) sandy silt with frequent thin layers of clay; (d) fine or medium sand. At the surface, the geological profile is completed by a layer of man-made soil (m) mainly consisting of coarse-grained material, sand and gravel with a thickness variable between about 3 and 15 m.

It is easy to infer that long-term settlements should be ascribed mainly to the most cohesive soils, i.e. lithotypes a and b, characterized by moderate to high compressibility, with compression index (Cc) varying between 0.24 and 0.35 (average value of 0.29) for the silty clay (a), and between 0.59 and 0.65 (average value of 0.63) for the organic silty clay (b) (Calabresi et al., 1980; Moscatelli et al., 2009; Pagliaroli & Moscatelli, 2013; Raspa et al., 2008).

The magnitude of the observed displacements can be linked both to the thickness of lithotypes a and b and to the age of buildings. Of course, the effects of the overloads on the most compressible layers decrease with depth.

Before considering in details the local heterogeneities of the alluvial deposits, it is worth noting that, despite a comparable thickness of the compressible layers, the cumulated settlements measured in S2 (ranging between about −20 and −30 mm) are significantly smaller than those of S1 (reaching about −70 to −80 mm).

This can be easily explained considering the age of the buildings: despite it is an area where the man-made soils have a thinner thickness, S1 has been urbanized starting from the southern part between the end of the 19th and the first half of the 20th centuries, while S2, which has a thicker layer of man-made soils, corresponds to the historical neighbourhood, built up from the roman age up to the 17th–18th centuries (Fig. 11).

To provide further insights on such a correlation, in this work four zones have been identified and deeply analysed, characterized by the


Fig. 13. Detailed view of the SBAS-DInSAR cumulative displacement map relevant to the area referred to as S2 in Fig. 2. The locations of the three selected buildings are also indicated.

Table 1
Overall statistics of the DInSAR results on the selected buildings: number of measurement points, average and minimum and maximum values of the annual velocity.

| Year of construction | Building | N. points | Average annual velocity (mm/year) | Min and max annual velocity (mm/year) |
|---|---|---|---|---|
| 1790-1815 | 1. Braschi | | | |
| 1650-1673 | 2. Altieri | | | |
| 1489/1848 | 3. Doria-Pamphili | | | |

Typical Soil Profiles (TSP), described in detail in Fig. 12, and indicated as TSP1 and TSP2 in Fig. 9 and TSP3 and TSP4 in Fig. 10, respectively.

By comparing first TSP1 (S1) with TSP4 (S2) and then TSP2 (S1) with TSP3 (S2), it is possible to note a similar stratigraphy for what concerns the thickness of the alluvial deposits, while the clay sequence is intercalated with sand in the TSP2–TSP3 case, only. Clearly, the settlement rates in correspondence to TPS2 and TPS3 are respectively smaller than those in TPS1 and TPS4, accounting for the lower thickness of the soft soils (lithotypes a and b) down to an about 30 metre depth, where the overloads are more effective. Besides, the larger displacements observed for TSP1 compared to TSP4 (which has a smaller thickness of the more compressible lithotype b), and for TSP2 compared to TSP3 should be ascribed to the more recent age of construction.

The obtained SBAS-DInSAR measurements, analysed in light of the geological setting and the spatial distribution of the settlements, indicate that the observed displacements are mainly linked to a residual consolidation process, correlated with the urbanization. The local variation in the deformation rates can be related to the thickness of very fine-grained soils and, especially, of organic soils filling the alluvial valley and to time since loading application. The building located in the ancient historical centre of Roma (S2 area) are relatively more stable (settlement rate about 1 mm/year), while most of the buildings constructed since the '50s (S1 area) are still affected by settlements about 3–4 mm/year.

## 6. Detailed DInSAR analysis on some buildings in the alluvial area

The S2 area includes the most valuable historical buildings of the town, which are in strict connection or, in some cases, built up on archaeological remains from the ancient Roman age. As discussed before, SBAS-DInSAR analysis does not evidence the presence of large settlements considering that the soil consolidation process should be already

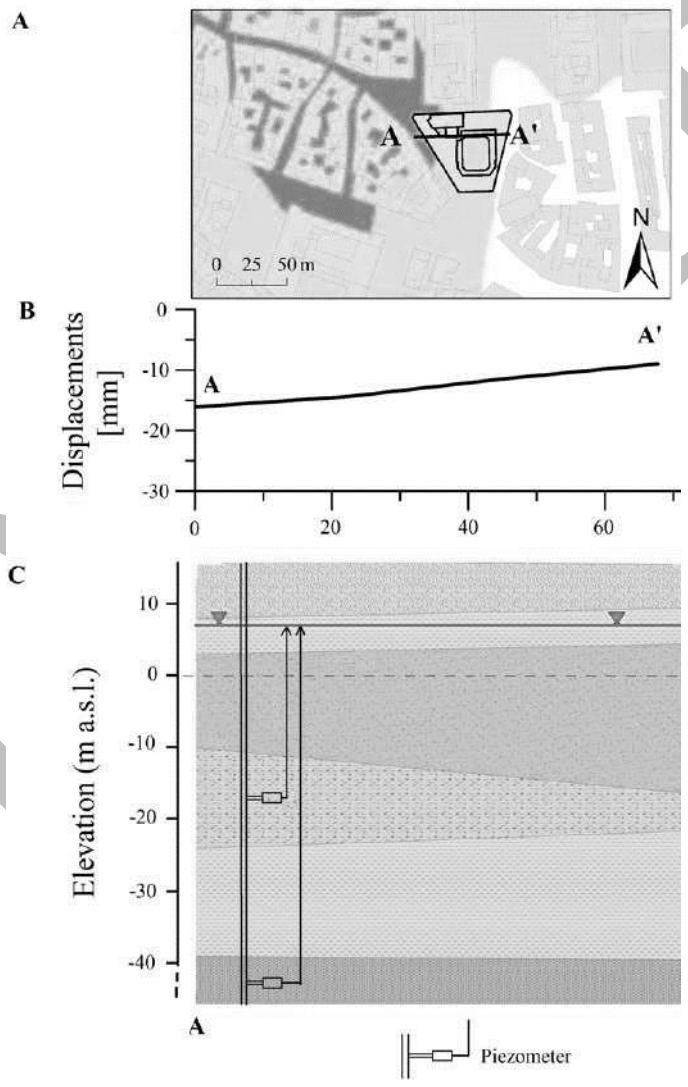


Fig. 14. A) Simplified plan of Palazzo Braschi (Bld. 1) superimposed on the contour map representing the cumulative displacements derived from the interpolation of the SBAS-DInSAR results; the trace of the analysed geological profile (AA′) is also reported; B) Trend of the cumulated displacement along the AA′ section; C) stratigraphic successions along the AA′ profile. The position of the piezometers located along the different layers is also depicted in C).

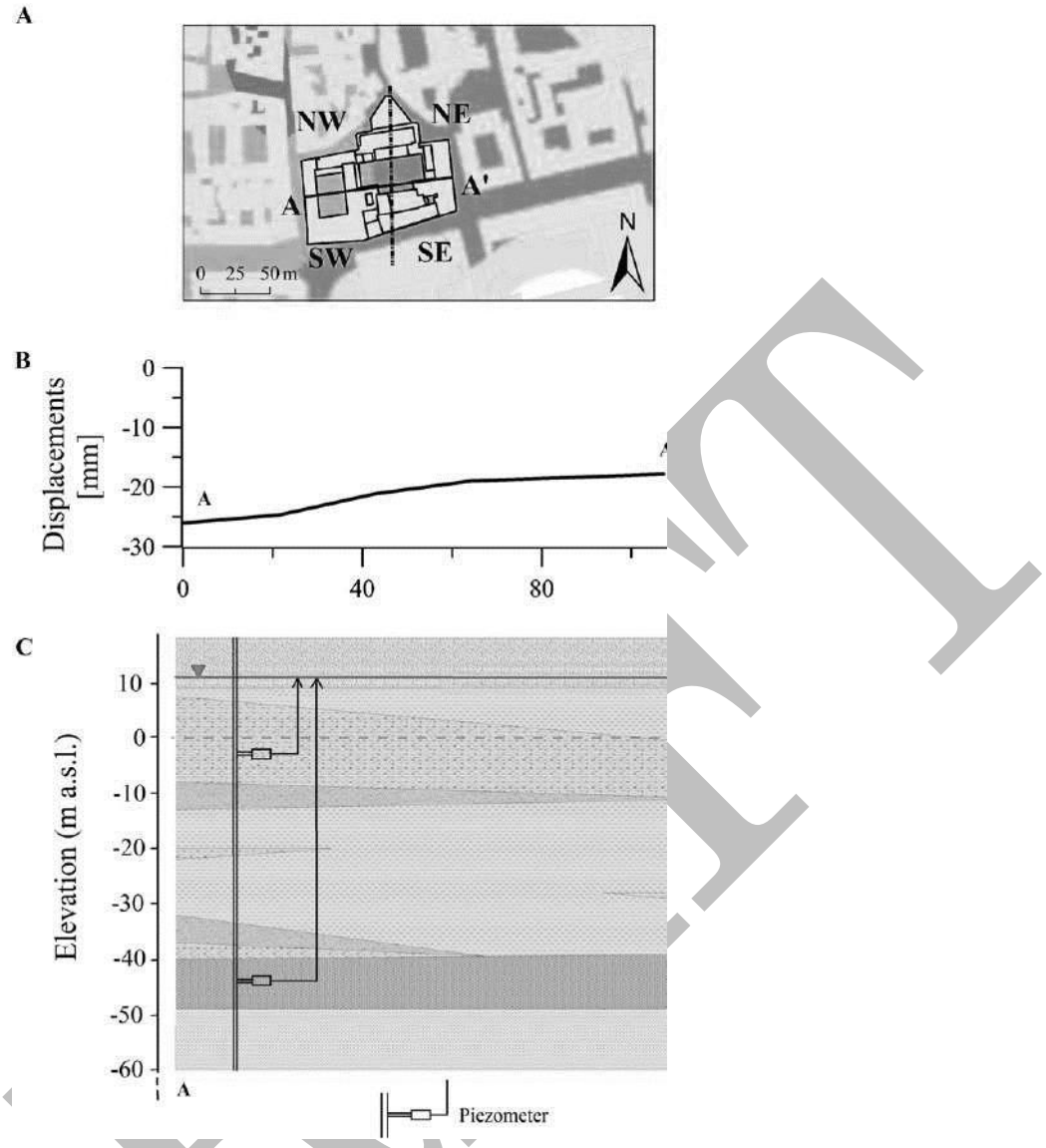


Fig. 15. A) Simplified plan of Palazzo Altieri (Bld. 2) superimposed on the contour map representing the cumulative displacements derived from the interpolation of the SBAS-DInSAR results; the trace of the analysed geological profile (AA') is also reported; B) trend of the cumulated displacement along the AA′ section; C) stratigraphic successions along the AA′ profile. The position of the piezometers located along the different layers is also depicted in C).

completed. However, by taking into account a very long observation period, it was possible to reveal the presence of small differential deformation trends on some buildings in this area. This analysis was conducted on three compounded buildings, where a sufficient number of coherent pixels provided quite reliable time series and average velocities larger than 1 mm/year.

The lateral and vertical variability of the less consistent alluvial layers can be correlated to different patterns of the settlements, accounted by a sufficient number of SBAS-DInSAR measurement points. These situations can lead to minor local instabilities, evidenced by cracking of parts of the structure, as well as to serious evolution, considering that most of the buildings are very ancient and deteriorated.

The analysed buildings, i.e., Palazzo Braschi, Palazzo Altieri and Palazzo Doria Pamphilj, which have been selected for their remarkable historical value, evidence different settlement characteristics, in terms of amplitude and spatial distribution of the observed deformation measurements, relevant to the 1992-2010 time interval. The analysis of the data available for the three buildings permitted to study and understand the causes of ground settlements. It is worth highlighting that this analysis is not trivial, since all the investigated buildings have heterogeneous structural characteristics, being the results of subsequent adaptations that combined ancient and modern constructions; moreover, they are often built up over previous archaeological remains. In Fig. 13 the location of the three selected buildings and the surrounding area, as well as the annual average velocities measured by the SBAS-DInSAR technique are shown. Table 1 summarizes the overall statistics of the results for each building.

Table 2
Overall statistics of the DInSAR results on Building 2 (Palazzo Altieri) grouped for sectors and time span: average annual velocity.

| Sector | Avg. vel (mm/year) | Avg. vel (mm/year) | | |
|---|---|---|---|---|
| | 1992-2010 | 1992-2000 | 2000-2005 | 2005-2010 |
| NE | −1.1 ± 0.3 | | | |
| NW | −1.3 ± 0.4 | | | |
| SW | −0.9 ± 0.4 | | | |
| SE | −1.2 ± 0.5 | | | |

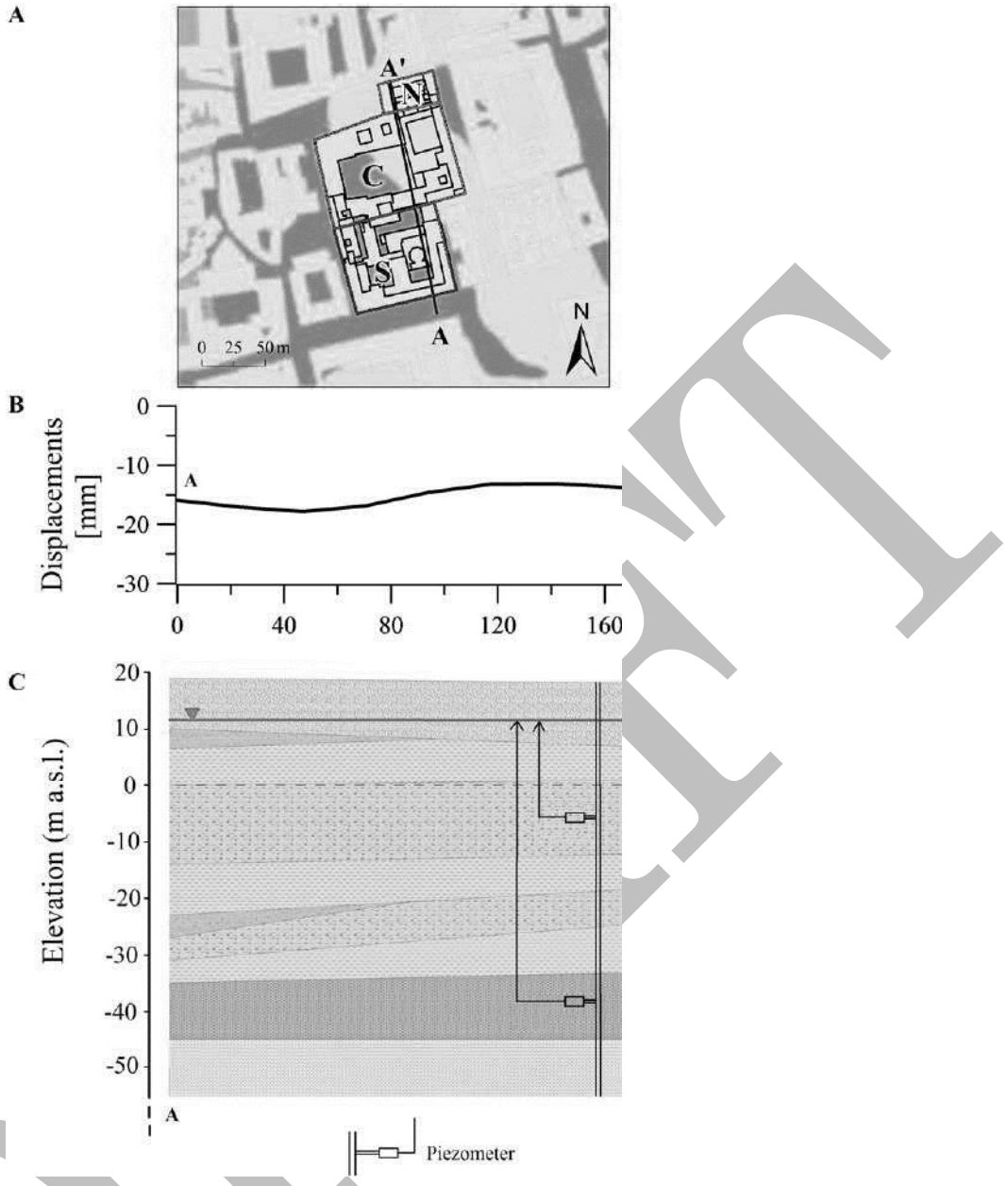


Fig. 16. A) Simplified plan of Palazzo Doria-Pamphili (Bld. 3) superimposed on the contour map representing the cumulative displacements derived from the interpolation of the SBAS-DInSAR results; the trace of the analysed geological profile (AA′) is also reported; B) trend of the cumulated displacement along the AA′ section; C) stratigraphic successions along the AA′ profile. The position of the piezometers located along the different layers is also depicted in C).

### *6.1. Palazzo Braschi*

Fig. 14 pictures a simplified plan of Palazzo Braschi, built up between 1791 and 1811, superimposed on the contour map representing the cumulative displacements derived from the interpolation of the SBAS-DInSAR results; moreover, a settlement profile (AA′) and the corresponding geological setting, as obtained along the stratigraphic profile cut along the same alignment, are also shown.

Table 3
Overall statistics of the DInSAR results on Building 3 (Palazzo Doria-Pamphili) grouped for different sectors: average annual velocity.

| Sector | Avg. vel (mm/year) |
|---|---|
| | 1992-2010 |
| N | |

The cumulative displacements (Fig. 14A) are on the average smaller than those observed for the other surrounding buildings ranging between. The analysis of the strati- graphic profile extrapolated in proximity of the building (Fig. 14C) evidences the presence of a thick layer of sand below the man- made soils, differently from other sites where we observe only clay layers. The thickness of the sand layer is thinner at the western side of the building (A) compared to the eastern side (A′). This trend is in accordance with the cumulative displacement profile (Fig. 14B) on the interpolated surface (Fig. 14A), showing that the displacements, cumulated over a 20-year observation period, de- crease where the sand layer is thicker.

### 6.2. Palazzo Altieri

Palazzo Altieri, built up between 1650 and 1676, is a large heterogeneous compounded building that has been modified and enlarged many times in the last centuries (northern side was built in 1734).

Therefore, the current structure shows relevant geometrical inconsistencies in the external facades and internal arrangements, as well as some portions of the foundations laying on pre-existing constructions. Fig. 15 shows the geological setting, obtained by exploiting the stratigraphic profiles derived from in field surveys in proximity of the building, and cumulative deformation measurements derived from the SBAS-DInSAR analysis.

The observed displacements are confined in the range between −18 and − 26 mm, which are significantly larger than those measured in correspondence to other buildings. Indeed, the stratigraphic succession (Fig. 15C), extrapolated in proximity of the building, shows that the succession below the man-made soils is composed, almost exclusively, by the more compressible layers, such as silty clay and organic silty clay, and that two thin sandy silt lens are only present in the western side of the geological profile.

The more compressible layer (organic silty clay) is shallower in the western side and its thickness decreases while proceeding toward the eastern side (A′), in accordance with the diminishing values of the cumulated displacement (curve AA′ in Fig. 15B).

To deeply investigate the possible correlation between constructive dis-homogeneities and ground settlements at local scale, a more detailed analysis of the SBAS-DInSAR time series was then performed. Such an analysis highlights that, despite a steady deformation trend corresponding to a total displacement of some mm between 1992 and 2010, distinct average velocities can be ob-tained for different observation periods and building sectors (Table 2).In particular, the displacement time series are grouped according to the four sectors of the building indicated in Fig. 15A (referred as NW, NE,SW, SE) and the corresponding average velocity is estimated for threedifferent time intervals, i.e. 1992–2000, 2000–2005 and 2005–2010 (Table 2). Over the whole time interval (1992-2010) the settlementsappear quite steady and comparable for all the selected building sectors, ranging from −0.7 to −2 mm/year. Along the NW and SE sectors, the time series highlight a slight increase of the velocities starting from 2000, probably due to localized cracking along the walls occurred after renovation works or to structural discontinuities among the different portions of the building.

Based on the above discussion, a simplified approach can be pursued to assess the possible damages related to the differential displacements, caused by soil-structure interactions. Cumulative displacements profile can be extrapolated along the specific alignments of the building facades, in order to evaluate the effects of bending forces, flexing the structure along its length, resulting in hogging (the structure curves upwards in the middle) and sagging (the structure curves downwards) zones. This information is strategic for the implementation of damage assessment model, to forecast the possible future critical evolution (Arangio et al., 2013).

### 6.3. Palazzo Doria Pamphili

Palazzo Doria Pamphili, built up between 1450 and 1507 and subsequently modified and enlarged in different phases between 1659 and 1890, is characterized by similar geological profiles but smaller displacement values with respect to those of Palazzo Altieri. This may be linked to the different age of construction of the considered buildings.

Fig. 16 summarizes the outcomes of the SBAS-DInSAR analysis in comparison with the geological profile along section AA′.

A simplified plan (which considers three zones N, C and S within the building) is shown in Fig. 16A, superimposed on the contour map representing the cumulative displacements derived from the interpolation of the SBAS-DInSAR dataset. The stratigraphic profile (Fig. 16C), extrapolated in proximity of the building, shows that, up to 30 m depth, the succession is substantially uniform and formed, almost exclusively, by the more compressible layers, such as silty clay and organic silty clay. On the contrary, slight variations in the curve of cumulated displacements are present (Fig. 16B) requiring further investigation.

As a matter of fact, Palazzo Doria Pamphili is an extremely complex and heterogeneous building compounded by distinct structures, differing in sizes and elevations, which were built up in different epochs and manners, and only recently unified in the present configuration. In order to take into account the effects of the age of construction, the average LOS displacement time series were estimated separately for the three sectors built up in different periods, which provided values that do not show significant differences over time (Fig. 16 and Table 3).

Thus the variation along the AA′ profile should be addressed to structural discontinuities between the different parts of the complex including also non-uniform foundations. The building is settled both in shallow portions (− 2.8 m below ground level) as well as in deeper ones (e.g. in the NW-SW sectors), with pillars reaching the clay level at about −12 m from the surface.

## 7. Conclusive remarks

The presented SBAS-DInSAR measurements retrieved through the 1992-2010 ERS/ENVISAT dataset show that, consistently with various results discussed in previous works, there is an on-going diffuse settlement process in correspondence to the buildings located in the areas of the town of Roma where the Tevere valley is filled by alluvial deposits of more recent formation. The retrieved SBAS measurements also show that since the last years, many buildings experienced ground settlements that are still on-going and even more evident on buildings of recent construction.

The joint exploitation of the long-term DInSAR deformation time series, the geological information and the structural characteristics of the buildings indicates that the observed displacement phenomena can be mainly linked to a residual consolidation process,. Additional factors, which influence the variation in the rate of settlements at a local scale, are related to local instabilities due to structural or foundation weaknesses. We also showed that the local variability in the subsidence rates can be ascribed to the intrinsic heterogeneity of the terrains forming the alluvial deposits. In addition, to evaluate the variation in magnitude of the settlements at a local scale, a more exhaustive analysis was conducted on some test cases by analysing stratigraphic profiles extrapolated along selected alignments. In particular, our study was deepened for three buildings, i.e. Palazzo Braschi, Palazzo Altieri and Palazzo Doria Pamphilj, located in the central part of Roma, East of the Tevere River.

Our analysis clearly showed that the magnitude of the settlements generally increases in light of a larger thickness of the more compressible layers. In addition, a local assessment of the magnitude of the cumulated displacements with respect to the thickness and distribution of the litho-stratigraphic successions was performed: lateral and vertical variations of the less consistent layers were correlated to different settlement patterns.

This kind of analysis permits to identify the areas where further geological and geo- technical surveys should be performed for supporting risk managementand mitigation activities. Moreover, it may play a key role in the contextof damage assessment analyses, because it may contribute to under- stand the static conditions of each building and to detect the weakest

segments that may require in-situ structural monitoring measurements or reinforcement actions. Further analyses are envisaged in order to exploit the long-term sequences of satellite data collected by higher spatial and temporal resolution SAR sensors, such as TerraSAR-X and COSMO-SkyMed constellations, because they may be crucial to detect very localized displacements in complex deformation scenarios.

## Acknowledgments

This work has partially been supported by the I-AMICA project (PONa3 00363). The analysed data were obtained in the framework of the project ESA-CAT1 N.6550 "ERS-ENVISAT full resolution deformation time-series in urban areas: the case of the city of Rome (Italy)". We also thank the NASA SRTM mission for the DEM relevant to the town of Roma.

## References

Amanti, M., Gisotti, G., & Pecci, M. (1995). I dissesti a Roma. In N. Accardi, R. Funiciello, & F. Marra (Eds.), *La geologia di Roma. Il Centro Storico. Memorie Descrittive della Carta Geologica d'Italia*, *vol. L*. (pp. 219-248).

Aquilina, C. (1937). Livellazione geometrica di precisione dei muraglioni del Tevere a Roma. *Annali dei Lavori Pubblici*, *9*, 1–16.

Arangio, S., Calò, S., Di Mauro, M., Bonano, M., Marsella, M., & Manunta, M. (2013). An application of the SBAS-DInSAR technique for the assessment of structural damage in the city of Rome. *Structure and Infrastructure Engineering: Maintenance, Management, Life-Cycle Design and Performance*. http://dx.doi.org/10.1080/15732479.2013.833949.

Ardizzone, F., Bonano, M., Giocoli, A., Lanari, R., Marsella, M., Pepe, A., ... Solaro, G. (2012). Analysis of ground deformation using SBAS-DInSAR technique applied to Cosmo-Skymed images, the test case of Roma urban area. *Proc. SPIE8536, SAR Image Analysis, Modeling, and Techniques XII, 85360D*. http://dx.doi.org/10.1117/12.979388 (November 21, 2012).

Berardino, P., Fornaro, G., Lanari, R., & Sansosti, E. (2002). A new algorithm for surface deformation monitoring based on small baseline differential SAR interferograms. *IEEE Transactions on Geoscience and Remote Sensing*, *40*, 2375–2383.

Bonano, M., Manunta, M., Marsella, M., & Lanari, R. (2012). Long-term ERS/ENVISAT deformation time-series generation at full spatial resolution via the extended SBAS technique. *International Journal of Remote Sensing*, *33*(15), 4756–4783. http://dx.doi.org/10.1080/01431161201163834O.

Bonano, M., Manunta, M., Pepe, A., Paglia, L., & Lanari, R. (2013). From previous C-band to new X-band SAR systems: Assessment of the DInSAR mapping improvement for deformation time-series retrieval in urban areas. *IEEE Transactions on Geoscience and Remote Sensing*, *51*(4), 1973–1984.

Bru, G., Herrera, G., Tomás, R., Duro, J., De la Vega, R., & Mulas, J. (2013). Control of deformation of buildings affected by subsidence using persistent scatter interferometry. *Structure and Infrastructure Engineering; Maintenance, Management, Life-Cycle Design and Performance*, *9*(2). http://dx.doi.org/10.1080/15732479201051971O.

Burgmann, R., Rosen, P. A., & Fielding, E. J. (2000). Synthetic aperture radar interferometry to measure Earth's surface topography and its deformation. *Annual Review of Earth and Planetary Science*, *28*, 169–209.

Burland, J. B., & Wroth, C. P. (1974). Settlements on buildings and associated damage. *Proceedings of Conference on Settlement of structures, Cambridge BTS* (pp. 611–654).

Calabresi, G., Cassinis, C., & Nisio, P. (1980). *Influenza del regime del Tevere sul comportamento di un fabbricato monumentale adiacente.* Firenze: Associazione Geotecnica Italiana – XIV Convegno Nazionale di Geotecnica.

Cascini, L., Ferlisi, S., Fornaro, G., Peduto, D., & Manunta, M. (2007). Analysis of a subsidence phenomenon via DInSAR data and geotechnical criteria. *Rivista Italiana Di Geotecnica*, *04*(07), 51–59.

Casu, F., Manzo, M., & Lanari, R. (2006). A quantitative assessment of the SBAS algorithm performance for surface deformation retrieval from DInSAR data. *Remote Sensing of Environment*, *102*(3–4), 195–210. http://dx.doi.org/10.1016/jrse200601023.

Dixon, T., Amelung, F., Ferretti, A., Novali, F., Rocca, F., Dokka, R., ... Whitman, D. (2006). Subsidence and flooding in New Orleans. *Nature*, *441*, 587-588. http://dx.doi.org/10.1038/441587a (1 June 2006).

Ferretti, A., Prati, C., & Rocca, F. (2000). Non-linear subsidence rate estimation using permanent scatterers in differential SAR interferometry. *IEEE Transactions on Geoscience and Remote Sensing*, *38*, 2202–2212.

Ferretti, A., Fumagalli, A., Novali, F., Prati, C., Rocca, F., & Rucci, A. (2011). A new algorithm for processing interferometric data-stacks: SqueeSAR. *IEEE Transactions on Geoscience and Remote Sensing*, *49*, 3460–3470.

Frutaz, A. P., & Carte del Lazio, I-III (1972). *Roma, Istituto di studi romani.*

Gabriel, K., Goldstein, R. M., & Zebker, H. A. (1989). Mapping small elevation changes over large areas: Differential interferometry. *Journal of Geophysical Research*, *94*, 9183–9191.

Funiciello, R., Giordano, G., & Mattei, M. (2008). *Carta Geologica del Comune di Roma scala 1:50.000, Memorie Descrittive della Carta Geologica d'Italia.* Firenze: LXX, SELCA.

Lanari, R., Mora, O., Manunta, M., Mallorquí, J. J., Berardino, P., & Sansosti, E. (2004). A small baseline approach for investigating deformations on full resolution differential SAR interferograms. *IEEE Transactions on Geoscience and Remote Sensing*, *42*, 1377–1386.

Lanari, R., Casu, F., Manzo, M., & Lundgren, P. (2007). Application of the SBAS-DInSAR technique to fault creep: A case study of the Hayward fault, California. *Remote Sensing of Environment*, *109*(1), 20–28.

Lanari, R., Berardino, P., Bonano, M., Casu, F., Manconi, A., Manunta, M., ... Zeni, G. (2010). Surface displacements associated with the L'Aquila 2009 Mw 63 earthquake Central Italy: New evidence from DInSAR time series analysis. *Geophysical Research Letters*, *37*, L20309. http://dx.doi.org/10.1029/2010GL044780.

Manunta, M., Marsella, M., Zeni, G., Sciotti, M., Atzori, S., & Lanari, R. (2008). Two-scale surface deformation analysis using the SBAS-DInSAR technique: A case study of the city of Rome, Italy. *International Journal of Remote Sensing*, *296*, 1665-1684.

Marra, F., & Rosa, C. (1995). Stratigrafia e assetto geologico dell'area romana. In N. Accardi, R. Funiciello, & F. Marra (Eds.), *La geologia di Roma. Il Centro Storico. Memorie Descrittive della Carta Geologica d'Italia*, *vol. L* (pp. 49–113).

Massonnet, D., & Feigl, K. L. (1998). Radar interferometry and its application to changes in the Earth's surface. *Reviews of Geophysics*, *36*(4), 441–500.

Massonnet, D., Rossi, M., Carmona, C., Ardagna, F., Peltzer, G., Feigl, K., & Rabaute, T. (1993). The displacement field on the Landers earthquake mapped by radar interferometry. *Nature*, *364*, 138–142.

Massonnet, D., Briole, P., & Arnaud, A. (1995). Deflation of Mount Etna monitored by spaceborne radar interferometry. *Nature*, *375*, 567–570.

Matheron, G. (1963). Principles of geostatistics. *Economic Geology*, *58*, 1246–1266.

Ministero dei Lavori Pubblici (1901). *Atti della Commissione nominata per riferire sui danni ai muraglioni del Tevere.* Roma: Tipolitografia del Genio Civile.

Mora, O., Mallorquí, J. J., & Broquetas, A. (2003). Linear and nonlinear terrain deformation maps from a reduced set of interferometric SAR images. *IEEE Transactions on Geoscience and Remote Sensing*, *41*, 2243–2253.

Moscatelli, M., Pagliaroli, A., Marconi, F., Raspa, G., Folle, D., Stigliano, F., ... Leone, F. (2009). Definizione di un indice di suscettibilità al cedimento delle alluvioni pleistocenico oloceniche del Tevere nell'area di Roma - Risultati preliminari. *Atti del 3° Congresso Nazionale AIGA*. San Giovanni: Valdarno (AR).

Mroueh, H., & Shahrour, I. (2003). A full 3-D finite element analysis of tunnelling adjacent structures interaction. *Computers and Geotechnics*, *30*, 245–253.

Pagliaroli, A., & Moscatelli, M. (2013). *Progetto UrbiSit. Indirizzi e criteri per l'uso dei dati interferometrici nel monitoraggio dei movimenti di massa in area urbana.* IGAG–CNR (internal report).

Peltzer, G., & Rosen, P. A. (1995). Surface displacement of the 17 May 1993 Eureka Valley, California, earthquake observed by SAR interferometry. *Science*, *268*, 1333–1336.

Raspa, G., Moscatelli, M., Stigliano, F., Patera, A., Marconi, F., Folle, D.-, ... Milli, S. (2008). Geotechnical characterization of the upper Pleistocene–Holocene alluvial deposits of Roma (Italy) by means of multivariate geostatistics: Cross-validation results. *Engineering Geology*, *101*, 251–268.

Sagnotti, L., Mattei, M., Faccenna, C., & Funiciello, R. (1994). Paleomagnetic evidence for no tectonic rotation of the central Italy Tyrrhenian margin since Upper Pliocene. *Geophysical Research Letters*, *21*, 481–484.

Sanabria, M. P., Guardiola-Albert, C., Tomás, R., Herrera, G., Prieto, A., Sánchez, H., & Tessitore, S. (2014). Subsidence activity maps derived from DInSAR data: Orihuela case study. *Natural Hazards and Earth Science Systems*, *14*, 1341–1360.

Sansosti, E., Berardino, P., Bonano, M., Calò, F., Castaldo, R., Casu, F., ... Lanari, R. (2014). How second generation SAR systems are impacting the analysis of ground deformation. *International Journal of Applied Earth Observation and Geoinformation*, *28*, 1–11. http://dx.doi.org/10.1016/j.jag.2013.10.007.

Sciotti, M. (2010). *The project of the new underground Line C in Rome. Grantor, Roma Metropolitane Srl, General Contractor, Metro C SpA. Geologic and Hydrogeologic Report.* (internal report).

Stramondo, S., Bozzano, F., Marra, F., Wegmuller, U., Cinti, F. R., Moro, M., & Saroli, M. (2008). Subsidence induced by urbanisation in the city of Rome detected by advanced InSAR technique and geotechnical investigations. *Remote Sensing of Environment*, *112*(6), 3160–3172.

Tapete, D., Fanti, R., Cecchi, R., Petrangeli, P., & Casagli, N. (2012). Satellite radar interferometry for monitoring and early-stage warning of structural instability in archaeological sites. *Journal of Geophysics and Engineering*, *9*(2012), S10–S25.

Tesauro, M., Berardino, P., Lanari, R., Sansosti, E., Fornaro, G., & Franceschetti, G. (2000). Urban subsidence inside the city of Napoli (Italy) observed by satellite radar interferometry. *Geophysical Research Letters*, *27*(13), 1961–1964.

Tizzani, P., Battaglia, M., Zeni, G., Attori, S., Berardino, P., & Lanari, R. (2009). Uplift and magma intrusion at Long Valley caldera from InSAR and gravity measurements. *Geology*, *37*(1), 63–66. http://dx.doi.org/10.1130/G25318A.1.

Tomás, R., Herrera, G., Delgado, J., Lopez-Sanchez, J. M., Mallorquí, J. J., & Mulas, J. (2010). A ground subsidence study based on DInSAR data: Calibration of soil parameters and subsidence prediction in Murcia City (Spain). *Engineering Geology*, *111*(1), 19–30.

Tomás, R., García-Barba, J., Cano, M., Sanabria, M. P., Ivorra, S., Duro, J., & Herrera, G. (2012). Subsidence damage assessment of a gothic church using Differential Interferometry and field data. *Structural Health Monitoring*, *11*(6), 751–762.

Trasatti, E., Casu, F., Giunchi, C., Pepe, S., Solaro, G., Tagliaventi, S., ... Lanari, R. (2008). The 2004-2006 uplift episode at Campi Flegrei caldera (Italy): Constraints from SBAS-DInSAR ENVISAT data and Bayesian source inference. *Geophysical Research Letters*, *35*, L073078. http://dx.doi.org/10.1029/2007GL033091.

Ventriglia, U. (2002). *Geologia del territorio Comune di Roma.* Servizio Geologico, Difesa del Suolo - Provincia di Roma.

Ventriglia, U., & Sciotti, M. (1970a). *Geological map of Rome.* (Florence, Italy).

Ventriglia, U., & Sciotti, M. (1970b). *Geological map of Rome. Man-made soils thickness.* (Florence, Italy).

Werner, C., Wegmüller, U., Strozzi, T., & Wiesmann, A. (2003). Interferometric point target analysis for deformation mapping. *Proc. of IGARSS, Toulouse, France, 2003* (pp. 4362-4364) (7).

Zebker, H. A., & Villasenor, J. (1992). Decorrelation in interferometric radar echoes. *IEEE Transactions on Geoscience and Remote Sensing*, *30*(5), 950–959.

Zeni, G., Bonano, M., Casu, F., Manunta, M., Manzo, M., Marsella, M., ... Lanari, R. (2011). Long term deformation analysis of historical buildings through the advanced SBAS-DInSAR technique: The case study of the city of Roma Italy. *Journal of Geophysics and Engineering*, *8*, S1. http://dx.doi.org/10.1088/1742-2132/8/3/S01.